Agricultural and Forest Meteorology 182–183 (2013) 43–53

Contents lists available at ScienceDirect

Agricultural and Forest Meteorology

journal homepage: www.elsevier.com/locate/agrformet

An operational model for forecasting ragweed pollen release and dispersion in Europe

Marje Prank[a,*], Daniel S. Chapman[b], James M. Bullock[c], Jordina Belmonte[d], Uwe Berger[e], Aslog Dahl[f], Siegfried Jäger[e], Irina Kovtunenko[g], Donát Magyar[h], Sami Niemelä[a], Auli Rantio-Lehtimäki[i], Viktoria Rodinkova[j], Ingrida Sauliene[k], Elena Severova[l], Branko Sikoparija[m], Mikhail Sofiev[a]

[a] Finnish Meteorological Institute, Finland
[b] Centre for Ecology and Hydrology, Edinburgh EH26 0QB, UK
[c] Centre for Ecology and Hydrology, Benson Lane, Wallingford OX10 8BB, UK
[d] Universitat Autònoma de Barcelona, Spain
[e] Medical University of Vienna, Department of Oto-Rhino-Laryngology, Austria
[f] University of Gothenburg, Sweden
[g] Institute for Hygiene and Medical Ecology, Ukraine
[h] National Institute of Environmental Health, Hungary
[i] University of Turku, Finland
[j] Vinnitsa National Pirogov Memorial Medical University, Ukraine
[k] Siauliai University, Lithuania
[l] Moscow State University, Russia
[m] University of Novi Sad Faculty of Sciences, Serbia

ARTICLE INFO

Article history:
Received 31 May 2013
Received in revised form 10 July 2013
Accepted 13 August 2013

Keywords:
Pollen dispersion modelling
Allergenic pollen forecasting
Ambrosia artemisiifolia L

ABSTRACT

The paper considers the possibilities of modelling the release and dispersion of the pollen of common ragweed (*Ambrosia artemisiifolia* L.), a highly allergenic invasive weed, which is spreading through southern and central Europe. In order to provide timely warnings for the allergy sufferers, a model was developed for forecasting ragweed pollen concentrations in the air. The development was based on the system for integrated modelling of atmospheric composition (SILAM) and concentrated on spatio-temporal modelling of ragweed flowering season and pollen release, which constitutes the emission term.

Evaluation of the new model against multi-annual ragweed pollen observations demonstrated that the model reproduces well the main ragweed pollen season in the areas with major plant presence, such as the Pannonian Plain, the Lyon area in France, the Milan region in Italy, Ukraine and southern Russia. The predicted start of the season is mostly within 3 days of the observed for the majority of stations in these areas. The temporal correlation between modelled and observed concentrations exceeds 0.6 for the bulk of the stations.

Model application to the seasons of 2005–2011 indicated the regions with high ragweed pollen concentrations, in particular the areas where allergenic thresholds are exceeded. It is demonstrated that, due to long-range transport of pollen, high-concentration areas are substantially more extensive than the heavily infested territories.

© 2013 The Authors. Published by Elsevier B.V. Open access under CC BY-NC-ND license.

1. Introduction

Common ragweed (*Ambrosia artemisiifolia* L.) is an annual weed native to the temperate regions of North America. Ragweed is a successful colonizer, and it is invasive in Europe, Asia and Australia (GISD, 2013). The preferred habitats of common ragweed include agricultural areas and regions with disturbed soil, such as wastelands, roadsides and urban areas (Bassett and Crompton, 1975). Its presence is considered harmful for a range of sectors, including human health, agriculture, biodiversity and the environment (Bullock et al., 2012). Among these, the human health impact due to allergy triggered by ragweed's wind-dispersed pollen is arguably the most important. Ragweed pollen has been recognized as a significant cause of hayfever and asthma (D'Amato et al., 2007). Among European allergy sufferers, sensitization to ragweed pollen ranges

* Corresponding author. Tel.: +358 295395472.
E-mail address: marje.prank@fmi.fi (M. Prank).

0168-1923 © 2013 The Authors. Published by Elsevier B.V. Open access under CC BY-NC-ND license.
http://dx.doi.org/10.1016/j.agrformet.2013.08.003

from 2.5% in Finland up to 60% in Hungary (Burbach et al., 2009). Pollen concentrations as low as 5–20 pollen grains per m^3 have been reported to be sufficient for sensitized patients to show symptoms (Oswalt and Marshall, 2008).

As common ragweed reproduces only by seeds, which are too large to be transported far by wind, the most important invasion pathways are related to human activities, such as seed import from infested areas and transport of contaminated soil by agricultural machinery (Bullock et al., 2012). Common ragweed has been repeatedly introduced to Europe since the 19th century through seed import from USA and Canada (Chauvel et al., 2006). However, ragweed has noticeably expanded since the middle of the 20th century, establishing self-sustaining colonies in European regions with favourable climatic conditions (Chauvel et al., 2006; Essl et al., 2009).

Hungary is the most infested European country (Makra et al., 2005; Pinke et al., 2011), though significant ragweed populations are also reported in Croatia (Peternel et al., 2006), Serbia (Šikoparija et al., 2009), south-eastern France (Laaidi et al., 2003a), and Northern Italy (Ridolo et al., 2006). Ragweed is also found in Bulgaria (Yankova et al., 2000), Romania (Hodisan and Morar, 2008), Austria (Jäger, 2000), Switzerland (Taramarcaz et al., 2005), Czech Republic (Rybncek and Jäger, 2001), Slovakia (Bartková-Scevková, 2003), Sweden (Dahl et al., 2000), Poland (Piotrowska and Weryszko-Chmielewska, 2006), the Baltic states (Saar et al., 2000; Šaulienė et al., 2011), Spain (Fernández-Llamazares et al., 2012) and in other countries including Germany and UK (Dechamp et al., 2009). There is little information about ragweed presence in the former Soviet Union; available data suggest that the largest European colony is established over Southern Ukraine, the Crimea Peninsula (Rodinkova et al., 2012; Simpson, 2011; Turos et al., 2009) and adjacent parts of Russia, (Reznik, 2009; Severova and Volkova, 2012; Vinogradova et al., 2010).

Quantitative mapping of ragweed habitat has been attempted for limited areas (Dechamp and Meon, 2009; Skjøth et al., 2010; Zink et al., 2012). However, on European scale the information on common ragweed presence has been largely qualitative (e.g. Delivering Alien Invasive Species Inventories for Europe (DAISIE, http://www.europe-aliens.org); Global Biodiversity Information Facility (GBIF, http://www.gbif.org), and (Dechamp et al., 2009)). Existing information about ragweed prevalence in the European Union has recently been synthesized into distribution maps at 10 and 50 km spatial resolutions (Bullock et al., 2012). However, the reliability of the ragweed occurrence information in Europe varies from region to region depending on the extent and availability of local reports. This is especially problematic for ragweed, where a single grid cell record in a highly infested area, such as Hungary, likely represents a large invasive population, while a record in northern Europe likely represents a few casual individuals arising from accidental introduction with imported seed (Bullock et al., 2012).

Airborne pollen observations provide an efficient way to improve the inventories by giving a better indication of local population sizes and potential health impacts. This approach has given acceptable results for other allergenic species, such as birch, grass and olive (Pauling et al., 2012; Rouïl et al., 2009, 2008; Sofiev et al., 2006). Apart from compensating for missing data and errors in the inventories, calibration using pollen counts also accounts for spatio-temporal variation in pollen productivity of the plants related to climatic and habitat factors. As an alternative approach, ecological models have been used to predict the invasion of the plant to suitable habitats (Bullock et al., 2012; Chen et al., 2007; Cunze et al., 2013; Smolik et al., 2010).

The phenological development of common ragweed (i.e. the timing of the pollen season) is another critical factor in modelling of pollen dispersion. A photothermal model for common ragweed phenology was suggested by Deen et al. (1998). This model is closely analogous to thermal-sum models, but also takes into account that ragweed is a short-day plant, i.e. its flowering can only start after the summer solstice, when the photoperiod is reduced below 14.5 h. The model was developed for multi-species competition simulations (Deen et al., 2001) and its predictions for timing of later phenological phases such as flowering have not been validated for naturally growing populations. The duration of the flowering season is not predicted by Deen's model. It has been suggested to be also largely driven by photoperiod; in the northern and mountainous areas it can also be terminated by frost (Dahl et al., 2000).

The flowering season is in August–September and a single ragweed plant can produce billions of pollen grains (Fumanal et al., 2007; Šaulienė et al., 2012). Pollen production depends on the size of the plant at the beginning of flowering (Basky and Magyar, 2008; Fumanal et al., 2007), which in turn depends on resources available during the growth season (solar radiation, CO_2, water, and nutrients). Any stress due to low temperature or drought limits the size of the plants, and thus also their pollen production (Deen et al., 1998). Pollen emission from infested areas can also be influenced by agricultural or weed control practices, genetic variability among populations, etc. Some of these factors are constant in time, while others vary from year to year or depend on conditions during the growth season.

As for other wind pollinated plants, it has long been recognized (e.g. Raynor et al., 1970) that the majority of the released pollen grains are deposited within a few hundreds of metres from the source. However, the huge amounts of pollen grains released by the ragweed plants and the sensitivity of allergic people to very low concentrations make the long-distance transport of even a small fraction of the pollen important. Long-range transport is also facilitated by the comparatively small size of the pollen grains (18–22 μm in diameter (Taramarcaz et al., 2005)) and favourable atmospheric conditions during its flowering in the late summer: intense convective vertical mixing lifts up the grains and mixes them rapidly through the whole boundary layer (Šikoparija et al., 2013).

Lack of information on the habitat has been the main obstacle to development of ragweed pollen dispersion models. The most comprehensive regional simulations to-date have been reported by Zink et al. (2012). That study used the COSMO-ART meteorological and dispersion model and combined it with a manually harmonized inventory of ragweed habitat in Germany, Austria, Czech Republic and Hungary. However, the model was applied only to a single short episode and the authors do not describe any phenological model to provide the timing of the flowering. In the USA, a model combining SILAM and COSMO-Art birch pollen source parameterizations (Helbig et al., 2004; Sofiev et al., 2013) has been applied to ragweed dispersion by Efstathiou et al. (2011). Various statistical models have also been used for predicting ragweed pollen season at specific locations (Laaidi et al., 2003b; Makra et al., 2012, 2011; Stark et al., 1997). However, no model simulations have so far covered the whole of Europe together with the eastern ragweed colonies in Ukraine and Southern Russia. Coverage of all the main source areas is necessary to represent accurately the role of long-range transport in forming the pollen patterns over Europe. The importance of long range transport is supported by numerous source apportionment studies which have applied inverse modelling to explain high pollen concentrations observed far from the infested areas (Belmonte et al., 2000; Buters et al., 2012; Efstathiou et al., 2011; Fernández-Llamazares et al., 2012; Galan et al., 2013; Ranta et al., 2011; Šikoparija et al., 2013, 2009; Smith et al., 2008; Stach et al., 2007), see also Chapter 5 of Sofiev and Bergmann (2013).

The features of ragweed described above – high pollen production, comparatively small size of pollen grains and summer environmental conditions facilitating long-range dispersion, as

well as low allergy triggering threshold and high sensitization among the European population – indicate the need for a European-scale modelling effort for timely forecasts of airborne ragweed pollen concentrations. The goal of this paper is to present a new model for ragweed pollen release and dispersion over the European continent, to evaluate the system over recent years, and to present first estimates of European-wide ragweed pollen load.

2. Materials and methods

2.1. SILAM dispersion model

The development of the ragweed pollen dispersion model was based on the System for Integrated modeLling of Atmospheric coMposition (SILAM; http://silam.fmi.fi (Sofiev et al., 2013, 2008), which is a chemical transport model currently used in research and operational applications related to air quality (including pollen) and emergencies (http://www.gmes-atmosphere.eu, http://www.myair.eu). SILAM is equipped with source terms for birch, grass and olive pollen (Galan et al., 2013; Siljamo et al., 2013, 2008; Sofiev et al., 2013, 2006; Veriankaitė et al., 2009). Different types of phenological models are in use: thermal sum models for birch and olive and fixed calendar days for grasses. The release of pollen to the atmosphere is dependent on meteorological conditions (Siljamo et al., 2013; Sofiev et al., 2013). Other processes included in SILAM cover the whole atmospheric lifecycle of pollen after its release into the air: transport with air masses, turbulent mixing and removal by dry and wet deposition. Pollen is considered a chemically non-reactive aerosol, whose atmospheric dispersion only depends on the basic properties of the grains, such as their aerodynamic diameter and density.

2.2. Input data

The habitat maps used for modelling total pollen production are among the most crucial and arguably most uncertain parts of the model input. For birch, grass, and olive these maps originated from land-use, forest, and agriculture inventories. Ragweed is the first species in SILAM for which the source term utilizes occupancy and climatic habitat quality maps from an ecological model. The model was applied to simulate the invasion of *A. artemisiifolia* in Europe, accounting for the climate suitability (temperature during the vegetative season, annual variations in temperature to break the dormancy, available moisture, etc.), seed import from infested areas, seed dispersal from invaded areas, and suitability of land use for ragweed. The maps were provided with spatial resolution of 5 km × 5 km. Both the underlying model and the ragweed habitat map are fully described in Bullock et al. (2012).

Meteorological information for the dispersion computations was obtained from the operational archives of the European Centre of Medium-range Weather Forecasts (ECMWF; http://www.ecmwf.int). The period considered in the study – from 2005 to 2011 – is covered with spatial resolution varying from 40 km (2005) to 16 km (2011)), depending on the version of the operational ECMWF model at the time. The bulk of the period (2006–2010) is covered with 25 km resolution. The time step between the meteorological fields was 3 h, with linear interpolation used to obtain the values for intermediate times.

For parameter identification and evaluation of the system the observational data of the European Aeroallergen Network (EAN; https://ean.polleninfo.eu/Ean) were used together with data from independent sources in Ukraine, Russia and Catalonia. EAN archives include ragweed pollen counts starting from 1974, for recent years covering Europe with over 250 stations. The network covers the Central European ragweed population and represents well the smaller colonies, such as the Rhône Valley in France, Northern Italy, Austria, etc. However, it has very limited coverage of the eastern colonies.

Table 1
Model parameters.

Logistic function of habitat climatic quality	
Middle point (a)	0.88
Slope (b)	−16.0
Maximum emission (E_{max})	1.5e7 pollen/m^2
Flowering start thresholds (2 sigma = 2.5%)	
Photoperiod	14.5 h
Bioday	25 ± 10%
Vegetation (bioday accumulation) start and flowering end (2 sigma = 97.5%) thresholds	
Photoperiod	12.0 h
Daily mean temperature	7.5 C
Instant temperature	0.0 C
Bioday accumulation	
Minimum temperature	0.9 C
Maximum temperature	40 C
Optimal temperature	31.7 C
Maximum optimal photoperiod	14.5 h
Pollen release (diurnal variations – bimodal normal distribution Martin et al., 2010)	
Peak 1 peak time (after sunrise)	135 min
Peak 2 peak time (after sunrise)	285 min
Peak 1 standard deviation	15 min
Peak 2 standard deviation	100 min
Fraction of pollen in peak 1	40%
Other parameters	
Pollen diameter	18 μm
Pollen density	800 kg/m^3
Emission injection height	ABL height

A limitation of the available pollen observations is that they cannot distinguish the pollen of *A. artemisiifolia* from other species of the *Ambrosia* genus. However, according to (Bullock et al., 2012; Makra et al., 2005), *A. artemisiifolia* is the most commonly occurring species in Western Europe and the Pannonian Plain and the ranges of the other *Ambrosia* species lie within that of *A. artemisiifolia*; a finding which is also supported by the population genetic data of (Mátyás and Vignesh, 2012). *A. artemisiifolia* is also the main and the most abundant species of ragweed in the south of Russia (Vinogradova et al., 2010). Although the uncertainty is higher for the Eastern colony in Ukraine and Russia, these data justify the use of the *Ambrosia* pollen counts for the model development and validation.

3. Development of the ragweed pollen emission model

This section describes the developments in SILAM to model ragweed. These developments were concentrated on the emission module, whose components are described below. A summary of the parameterization can be found in Table 1.

3.1. Predicting the timing of the flowering

A comprehensive model for predicting the timing of ragweed phenological phases was suggested by Deen et al. (1998). The authors suggest 'biodays' as the main driving parameter, and these combine the effects of temperature and photoperiod on ragweed development rate. As this model only covers the phenological phases after the breaking of seed dormancy, an assumption needs to be made about the timing of the dormancy break and the beginning of the growing season, when the bioday accumulation starts. In SILAM, seed dormancy is broken when the daily mean temperature exceeds 7.5 °C and no more frosts occur, but not earlier than the spring equinox, as light is an important factor to start germination (Baskin and Baskin, 1980).

Although too long photoperiod slows down phenological development in Deen's model, this does not delay the pollen season sufficiently in southern areas, and leads to an unrealistically early initiation of flowering: the suggested flowering initiation threshold of 25 biodays is reached in June. This problem can be overcome by adding another threshold – the shortening of the photoperiod below 14.5 h – that has to be reached to initiate flowering. This threshold is reached at the beginning of August, which corresponds well with the season observed in the main ragweed colonies in Eastern and South-eastern Europe and is consistent with ragweed's 'short day' nature.

If both thresholds are applied, flowering in warm regions is initiated by the shortening of day length, while in the regions with insufficient heat accumulated by August, the plants delay the flowering until the 25 biodays threshold is reached. In Europe, the transition from one criterion to another would take place around 50° N latitude (southern England, central Germany and Poland). The bioday threshold can also delay the flowering in mountainous regions.

Deen's phenology model does not predict the end of the flowering season. Other studies suggest that, in a similar way to the start of the flowering, the season end also depends on several parameters; in southern areas it is controlled by shortening of the photoperiod, while in the north the flowering is ended by low temperatures and the occurrence of first frosts (Dahl et al., 2000; Ziska et al., 2011). Based on airborne pollen observations in Europe, the same threshold values that govern the start of the growth season in spring (12 h photoperiod, daily mean temperature below 7.5 °C or occurrence of frosts) can be applied to end flowering in autumn.

3.2. Flowering during the season

The inflorescences of common ragweed consist of many individual flowers that reach anthesis sequentially. Pollen release from a single flower lasts only up to 6 h (Martin et al., 2010). In SILAM the pollen emission from a certain area is considered as a stochastic process, whereby all the individual flowers follow the mean phenological model but with slight deviations. The probability distribution of flowering is assumed to be Gaussian, centred midway between the start and end dates of the flowering season determined by the thresholds discussed in Section 4.1. The length of the season determines the width of the flowering distribution function, corresponding to two standard deviations of the Gaussian distribution. This corresponds to one of the commonly used definitions of the start and the end of a pollen season (listed in Jato et al. (2006)) as the respective dates when 2.5% and 97.5% of the total seasonal pollen count are reached.

The process of pollen emission from a single ragweed flower and its temporal evolution is described by Martin et al. (2010). Following the observations presented in that paper, the diurnal variation in pollen release intensity is described in SILAM as a bimodal normal distribution (parameters are given in Table 1).

3.3. Total amount of pollen emitted during the season

The fraction of a model grid cell occupied by ragweed is obtained by multiplying the fraction of suitable land use types (agricultural and anthropogenic) in the area with the probability of ragweed occupancy from the ecological model. The amount of pollen emitted during a season by a unit area fully covered by the plant is assumed to be a logistic function of the climatic habitat quality index computed by the ecological model (taking values between 0 and 1). The total emission from a grid cell is

$$E_{total} = \frac{A * LU_{fraction} * Occ * E_{\max}}{1 + e^{a*(Q-b)}}$$

Here E_{total} [#] is the amount of pollen emitted by a model grid cell with area A [m^2] during the whole flowering season; $LU_{fraction}$ is the fraction of the area under suitable land use, Occ is the probability of ragweed occupancy from the ecological model [relative], E_{max} [#/m^2] is the pollen emission *per* unit area under ideal conditions, and Q is the climatic habitat quality index [relative]; a and b are coefficients of the logistic function (Table 1). Ragweed occupancy and habitat quality were gridded across Europe by Bullock et al. (2012); the maximum amount of pollen emitted *per* unit area and the coefficients of the logistic function were parameterized using the observations of airborne pollen concentrations.

3.4. Other parameters

The aerodynamic properties of ragweed pollen grains relevant for their dispersion and deposition are shown in Table 1. The ragweed pollen grain is assumed to be spherical with a characteristic diameter of 18–22 μm (Taramarcaz et al., 2005) and dry density of ~800 kg m^{-3} (Mandrioli et al., 2003). For simplicity, we assume no humidity dependence of pollen grain density.

It is assumed that the vertical injection profile of pollen emission is homogeneous within the atmospheric boundary layer, without any vertical gradient. This parameterization qualitatively reflects the process of turbulent mixing during one model time step (about 15 min for European scale simulations).

4. Model application and evaluation

4.1. Model setup

SILAM computations were made for a domain covering the whole area for which the ragweed occupancy data from the ecological model existed (17 W to 45 E; 30 N to 73 N). The horizontal resolution was 0.2° in both directions. The model vertical grid consisted of 8 uneven levels reaching up to ~7 km. The period 2005–2011 was chosen for the study. Computations were made with 15 min temporal resolution and the output consisted of hourly pollen emission and concentration maps. For comparison with the pollen observations, which were mainly available with daily resolution, time series were extracted from the model output at the station locations and averaged *per* day. SILAM data were screened for the missing observational information and only the days with existing monitoring data were included in the analysis.

4.2. Adjustment of the pollen emission map

Simulations with the ragweed pollen emission map obtained as described in Section 4.3 (Fig. 1, left-hand panel) through 2005–2011 resulted in mean total seasonal counts shown in Fig. 1, middle panel. The modelled pattern of ragweed pollen abundance over Europe, while in good agreement with observed totals (spatial correlation between observed and modelled totals is 0.74), does not match observations in certain regions. The right-hand panel of Fig. 1 shows the fractional bias of the modelled pollen concentration in the observation stations, defined as

$$FB = 2 * \frac{M - O}{M + O}$$

Here O is the observed and M is the modelled pollen concentration. As seen from this map, pollen concentrations in the eastern region (Ukraine, Russia) are strongly underestimated. Also the smaller colonies in France and Northern Italy are not accurately reproduced. Such 7-year mean biases in the model are most likely caused by uncertainties associated with the incomplete data describing ragweed presence across Europe. To reduce this bias and increase correspondence between the SILAM predicted seasonal total pollen

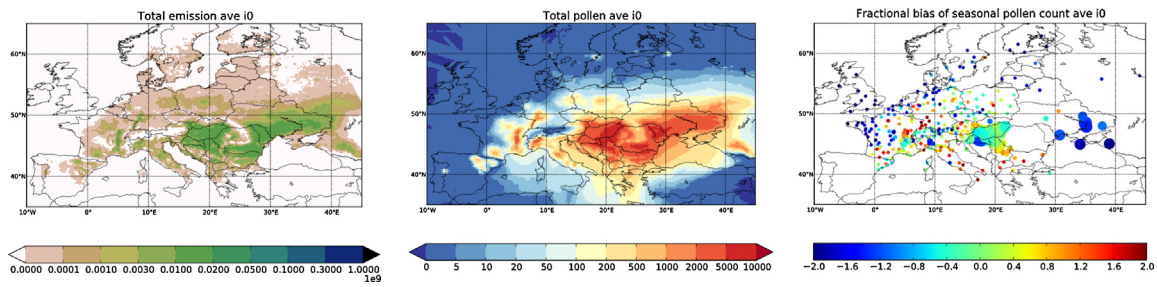

Fig. 1. Seasonal pollen emission [pollen m^{-2} $year^{-1}$] (left), total seasonal pollen count (sum of daily mean concentrations) [pollen m^{-3}] (middle) and fractional bias of the total pollen count [relative unit] (right) with initial emission, average 2005–2011. The size of the circles indicates the average ragweed pollen abundance in the area.

counts and the observed values, the initial map was corrected in the following way: first the ratio of the observed to the predicted total seasonal counts was calculated for observation sites and interpolated to a regular grid. Then the resulting map was used as a scaling factor for the initial source map and the model simulations were repeated. After three iterations, the 7 years mean total seasonal pollen counts were reproduced equally well in all main source regions (Hungary, Ukraine, Rhône valley in France, Northern Italy) (Fig. 2, right-hand panel) and the corrected emission map (Fig. 2, left-hand panel) was considered final. This procedure is similar to the source calibration in SILAM birch re-analysis of 2008–2010 (Rouïl et al., 2009, 2008) and is related to the simpler approaches of (Pauling et al., 2012; Skjøth et al., 2010), who directly used seasonal total counts to scale the distribution maps without any transport modelling. Such calibration of the emission map does not involve any change to model parameter values related to phenology, pollen release, etc.

Application of the correction increased the spatial correlation of seasonal totals across observational stations from 0.74 for uncorrected distribution map to 0.89. The resulting mean total seasonal pollen count is shown in the middle panel of Fig. 2. The highest amounts of pollen are present in the eastern colony north of Black Sea and on the Pannonian plain, and noticeable amounts are also shown in the Rhône valley in France and the Milan region in Northern Italy. The model reproduces the observed total seasonal pollen counts in the main source areas and in Central Europe without major bias (Fig. 2, right hand panel). The results show negative fractional bias in areas far from the sources, such as Great Britain and Scandinavia. In these areas the local emission is expected to be very small (Fig. 2, left hand panel) and the pollen counts there are also extremely low, though a few ragweed pollen grains are still occasionally observed.

The results discussed further are all based on the computations made using the corrected ragweed distribution.

4.3. Predictions of pollen season propagation

Using the model, the propagation of the flowering season can be determined from two proxies: pollen emission and its concentration in the air. The first proxy reflects phenological developments, while the second one corresponds to the pollen season as determined from airborne pollen observations. The upper row of Fig. 3 shows the propagation of the predicted flowering season based on pollen emissions and the lower row shows the propagation based on airborne pollen concentrations. The leftmost panels show the start date of the season based on the 2.5% threshold, the central panels – the date of mid-season, and the rightmost ones – the end of the season based on 97.5% of the seasonal total. Flowering starts in the south where the days get shorter most rapidly and gradually moves north, where it can also be delayed by the bioday threshold. The end of flowering happens synchronously all over Europe around the autumn equinox. The pollen season is longest in the main source regions – pollen counts reach 2.5% of the seasonal total earlier, and the 97.5% percentile later than elsewhere. The short, late-starting and early ending pollen season outside the source area is mainly due to the fact that the majority of pollen is brought there by long range transport episodes, which can only occur while the main source areas are flowering. In several countries, pollen monitoring stops before the end of the ragweed season, which obviously shortens the apparent duration of the season, both for observed and modelled time series (only days with existing observations were considered in the analysis).

The analysis of the observed and modelled pollen concentration time series shows that the model reproduces the season propagation in the western colony fairly well. A slight north–south gradient of model accuracy can be observed for the Pannonian Plain, where the season length is over-predicted by a couple of days in the south (northern Serbia) and under-predicted by 2–3 days in the north (northern Hungary, Fig. 4). As for the eastern colony, the observations are scarce with only one season or less reported by most of

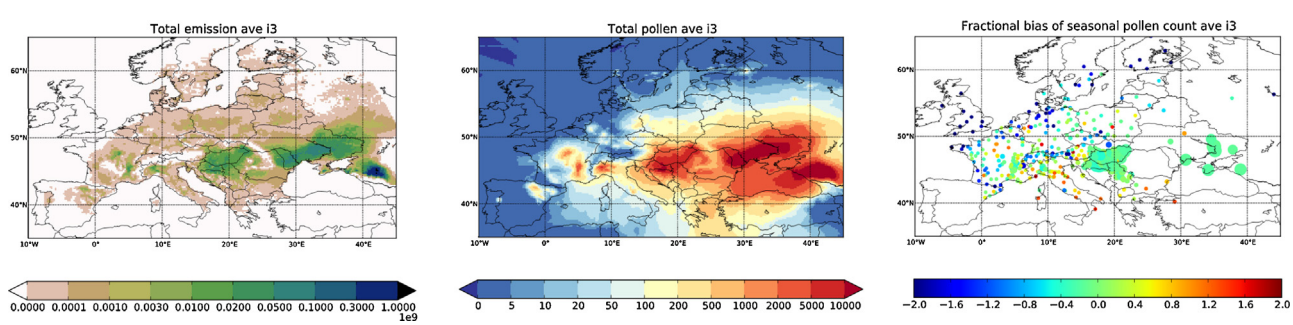

Fig. 2. Seasonal pollen emission [pollen m^{-2} $year^{-1}$] (left), total seasonal pollen count (sum of daily mean concentrations) [pollen m^{-3}] (middle) and fractional bias of the total pollen count [relative unit] (right) with corrected emission, average 2005–2011.

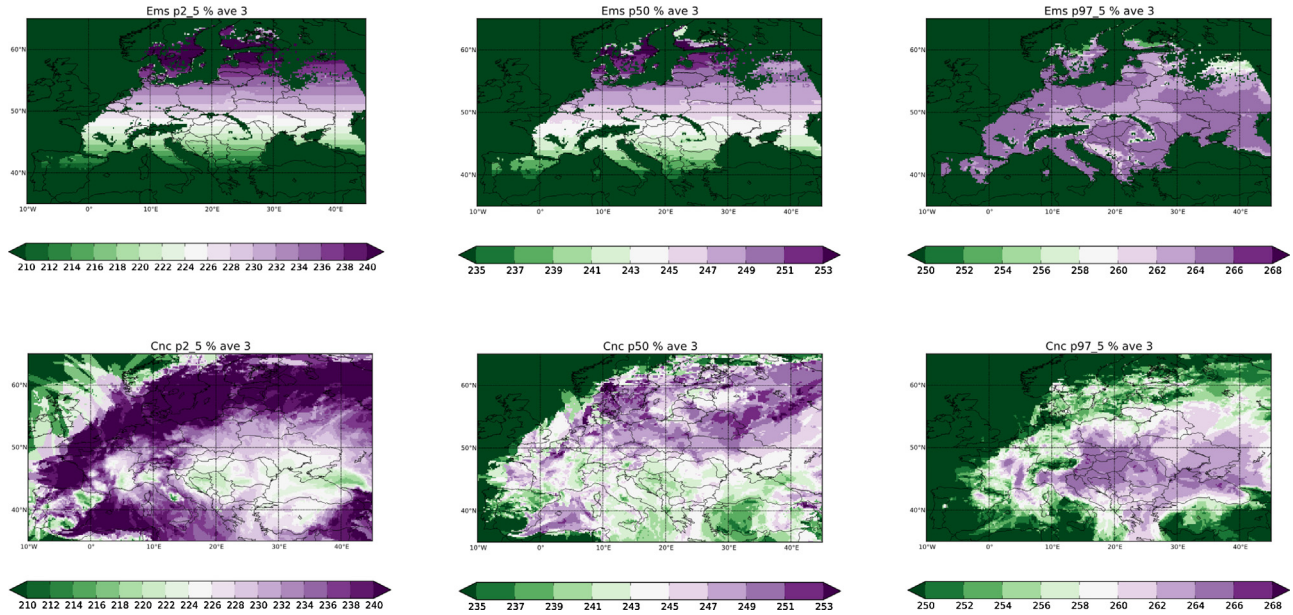

Fig. 3. Season progression [day of the year]: start (left), middle (centre) and end (right panels), calculated as 2.5%, 50% and 97.5% of seasonal pollen emission (upper row) or seasonal total count (lower row), respectively.

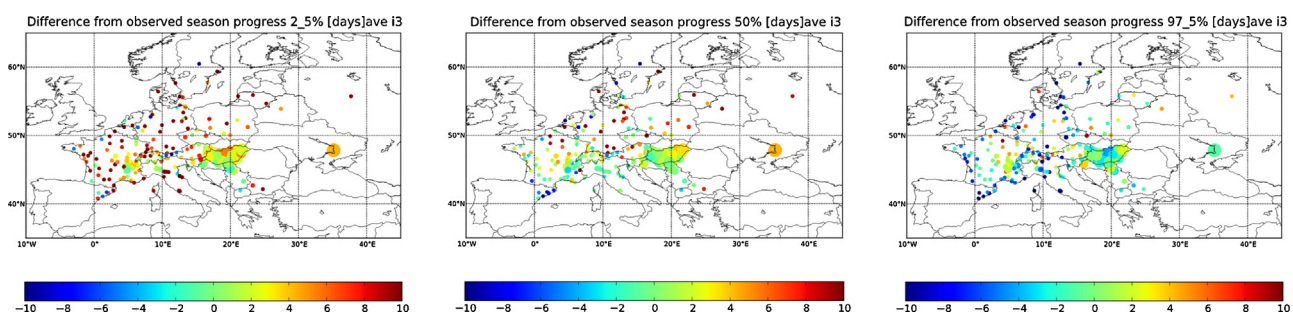

Fig. 4. Season progression accuracy – model-measurement difference [days], calculated from predicted and observed 2.5% (left), 50% (centre) and 97.5% (right) of seasonal pollen count. Only stations with at least 5 years of observations are plotted.

the stations; therefore the accuracy of the predictions cannot be reliably evaluated there.

The fraction of years in which the modelled start and end of the season differed by less than 3 days from the observed ones is plotted in Fig. 5. In the main source regions this accuracy is attained in most years and for a majority of the stations. On the Pannonian Plain the start of the season is reproduced better than the end; the opposite is true for the Rhône valley, the Milan region and Ukraine. For areas with lower ragweed infestation the results vary widely, owing to the much patchier local ragweed distributions, which cannot be reproduced.

The temporal correlation of modelled and observed seasonal time series is mostly above 0.4–0.5 in the main source regions (Fig. 6). The correlation values are low in areas without strong local emission in which the majority of observed pollen originates from poorly characterized patchy local sources and isolated peaks of long range transport.

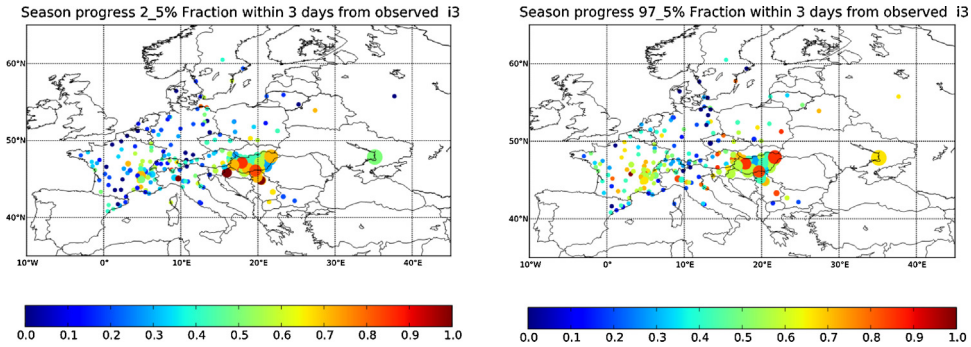

Fig. 5. Season progression accuracy – fraction of years when the modelled season start (left) or end (right) is within 3 days of the observed dates. Only stations with at least 5 years of observations are plotted.

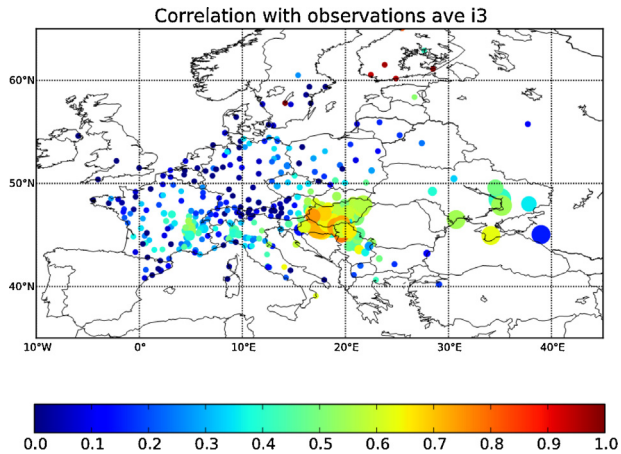

Fig. 6. Temporal correlation of observed and modelled seasonal time series, average 2005–2011.

Apart from the seasonal total count, the total duration of periods with concentrations exceeding certain health-relevant threshold levels was also computed. With no consensus on a single threshold in literature we selected 5, 20 and 100 pollen m^{-3} to reflect the range of the values from relevant publications collected in Table 4.3 in Bullock et al. (2012); although it should be noted that the lower threshold values of 5–20 m^{-3} are the more likely (Oswalt and Marshall, 2008). The predicted maps of average number of hours during a season during which ragweed pollen concentrations exceed these thresholds are shown in Fig. 7. Such maps cannot be evaluated directly since the observations are daily. As an indirect quality indicator, the number of days when the average concentration exceeds these thresholds was compared with the observed exceedances (Fig. 8). The agreement was very good in the main source regions – the predicted duration of exceedances differs from the observations by no more than 10%.

For the same thresholds, hit rates and false alarm ratios were computed (Fig. 9). The exceedances of the lower thresholds are reproduced with higher accuracy (only ~10% of false alarms and 80–90% of correctly predicted events) than the rarer exceedances of the highest threshold where the model tends to give more false alarms (up to 30% in some regions) and also misses up to half of the actual events.

5. Discussion

5.1. Ragweed pollen distribution pattern

Multi-annual simulations of ragweed pollen dispersion showed that, in general, the affected area is correlated with high-infestation regions. Thus, the highest pollen concentrations are predicted for Ukraine and the Pannonian Plain, with hot spots also in France and Northern Italy. However, high concentration areas are noticeably more extensive (compare left and middle panels in Fig. 2). As seen from Fig. 7, due to long-range transport allergy-relevant concentrations can occasionally occur nearly anywhere in Europe. Episode-wise, high concentrations (up to ~100 of pollen m^{-3}) can be measured thousands of kilometres away from the source areas (e.g., in north of Scandinavia – see Fig. 4 in Ranta et al. (2011)). Certain natural barriers still exist; pollen does not easily cross the Alpine ridges, Carpathian mountains or Pyrenees (Fig. 2, middle panel), which reduces the load in western Germany, Benelux, and Spain. Pollen spread is also evidently controlled by prevailing wind patterns. As a result, Eastern Ukraine is more strongly affected than the northern parts. The west-to-east direction of transport also explains the significant decrease of mean concentrations towards Northern Europe and comparatively low pollen levels in Scandinavia, as well as in the countries upwind of the main sources, such as the UK and Spain.

5.2. Model performance, main reasons for uncertainties

Evaluation of the model performance is one of the most crucial tasks while developing a new model. Ideally, every new model component should be validated independently. In the current case the new model components are the phenological model that predicts the flowering time and the ragweed habitat map. The timing of

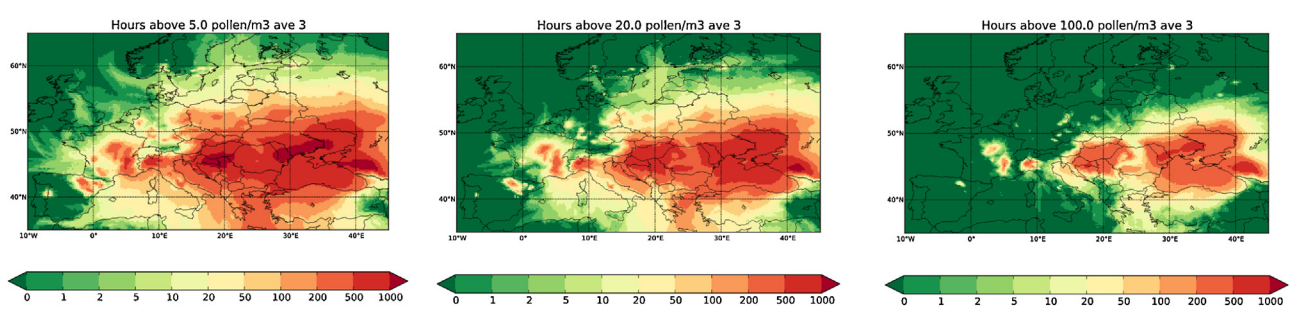

Fig. 7. Modelled hourly exceedances of 5 (left), 20 (middle) and 100 (right) pollen m^{-3} thresholds (total number of hours per season, average 2005–2011).

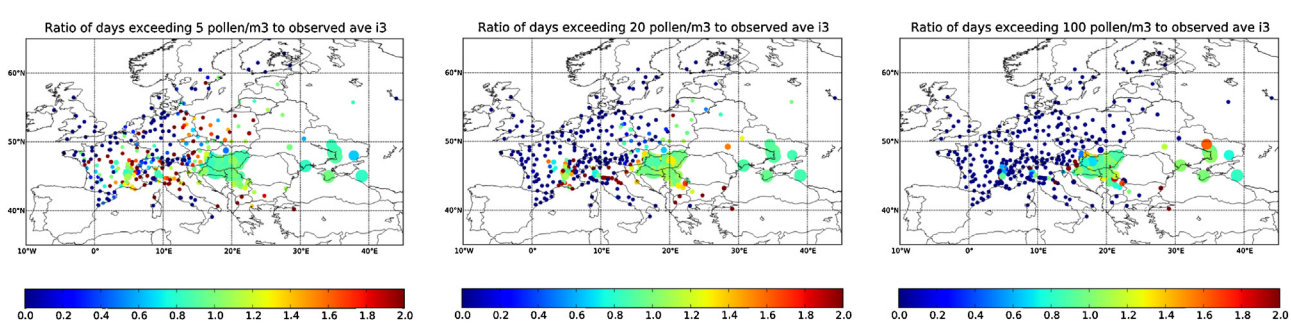

Fig. 8. Model-measurement ratios of daily threshold exceedances (same thresholds as in Fig. 7).

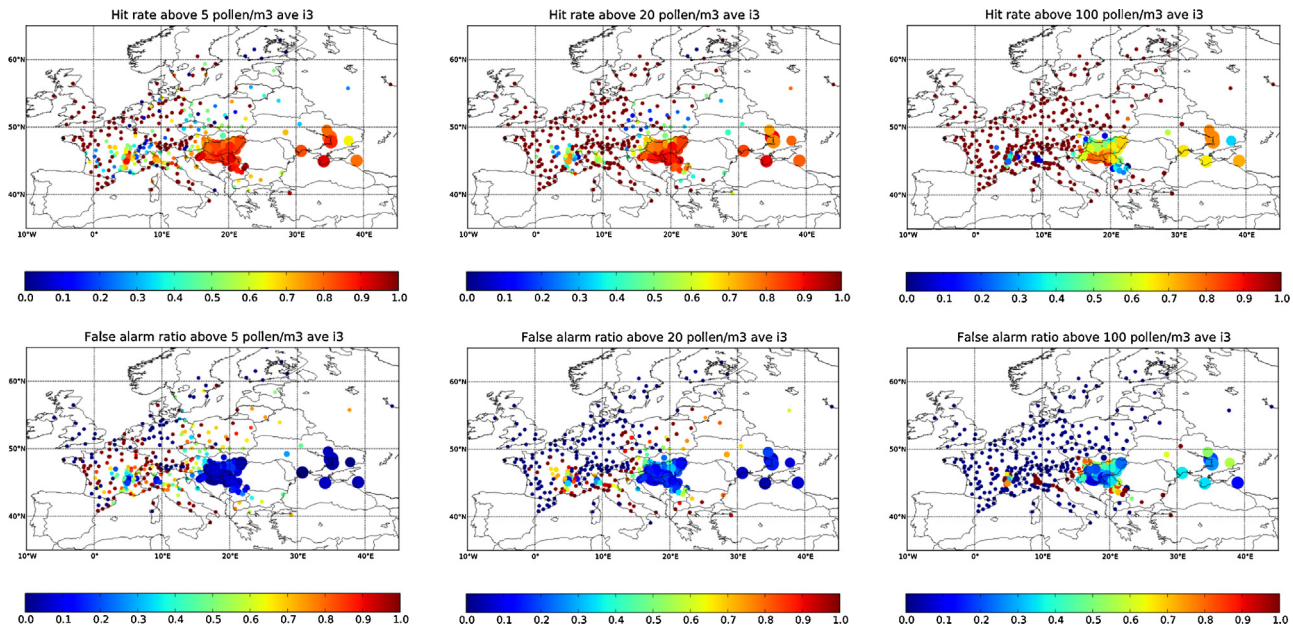

Fig. 9. Hit and miss statistics: upper panel – hit rate (fraction of correctly predicted exceedances out of all observed ones), lower panel – false alarm ratio (fraction of false alarms in all predicted exceedances) (same thresholds as in Fig. 7).

ragweed phenological phases is not regularly observed in Europe. In situ inventories of ragweed presence do exist, but, as shown by Bullock et al. (2012) and Cunze et al. (2013), large sampling bias makes such data hard to utilize. Therefore, essentially the only data regularly available over Europe for model validation are the airborne pollen observations. While these data allow only indirect validation of the individual model components, they can be used to evaluate the model as a whole. Thus, the obtained scores characterize the predicted airborne pollen distribution, which is the parameter relevant for allergy.

The SILAM model incorporates several processes, each of which is prone to uncertainties. Some of these, such as the uncertainty about ragweed habitat and its pollen production, were reduced using airborne pollen observations (Section 5.2). The others refer to phenological processes describing the growth season and the timing and intensity of the flowering. Most of these processes are described via a set of threshold values for heat accumulation, photoperiod and critical temperatures (Table 1).

Several parameters were collected from the available literature, which suggested, for instance, a 14.5 h day length threshold for flowering initiation (Deen et al., 1998). This value appeared to fit well with the airborne pollen observations. A contrasting example is the minimum of 25 biodays of heat accumulation suggested by Deen et al. (1998), which in our simulations appeared irrelevant for all the main ragweed areas; the required amount of heat is accumulated by June, which is much too early. This criterion plays a role only north of ~50° N latitude, where the lack of accumulated heat can delay the flowering start in the current model formulations. However, verification of this conclusion was not possible due to very low emissions in these regions.

The model sensitivity to some threshold values was high enough, so that they could be obtained via fitting the model results to the observed pollen concentrations. An example is the date of autumn equinox that appeared to represent well the end of the flowering season in southern regions. The sensitivity to some other parameters appeared to be less. In particular, the daily temperature threshold of 7.5 °C as an indicator of plant growth and first frosts as a cause of plant death, could be varied over a couple of degrees without major impacts on model performance. This is because in the major regions of pollen production growth and flowering are not limited by temperature but instead rely upon photoperiod.

The early end of pollen monitoring in some regions did not allow accurate calibration of the end of the flowering season in these areas. As ragweed has a late season compared to other European allergenic species, extending the pollen monitoring in these countries would provide valuable information. Short-term processes such as diurnal variation of the emission intensity could not be validated due to predominantly daily observations in the main source regions.

5.3. Calibration of the source map

The distribution of ragweed is among the most uncertain parts of the current model. The model used a predicted distribution map, with emissions scaled as a function of the modelled probability of invasion, climatic suitability and fraction of appropriate land-use (Bullock et al., 2012). The large uncertainty in this modelling arises from ragweed having a very widespread distribution (plants are recorded across nearly all parts of Europe), but only having established large populations in a subset of its range, such as the Pannonian Plain, the Rhône valley and northern Italy. Furthermore, the distribution data from some of the major pollen sources in Ukraine and Russia are very incomplete, which hindered the modelling of the invasion in these regions. To reduce the impact of this uncertainty on the results, the emission map was calibrated so that the total seasonal counts, averaged over 7 years, are predicted correctly. This procedure, however, has two caveats. Firstly, it attributes all systematic model errors to the emission term. Secondly, its efficiency is dependent on abundance of observations.

Systematic errors in the transport model originate from uncertainties in vertical mixing, deposition parameterization, quality of meteorological data, etc. In the current case, it is believed that such internal uncertainties are lower than those in the emission term. Indeed, the SILAM model has been extensively evaluated against air quality observations over Europe (Huijnen et al., 2010; Solazzo et al., 2012a,b; http://www.gmes-atmoshpere.eu). These generally confirm that the system has balanced setup with no clear pattern of regular biases in the main transport modules.

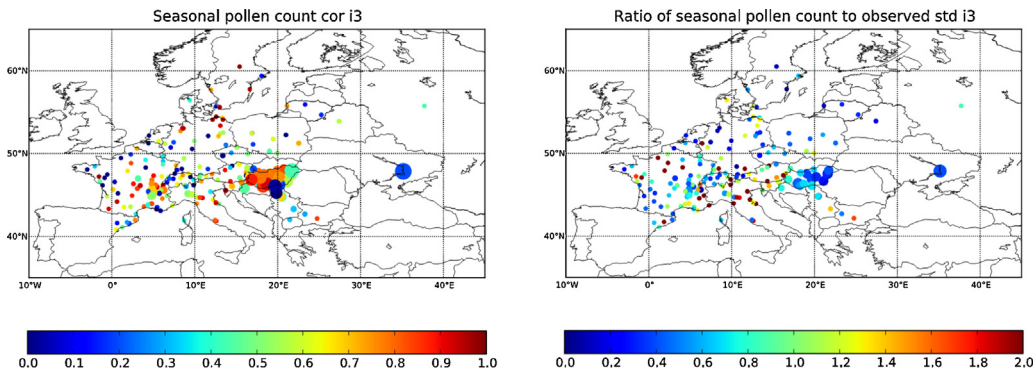

Fig. 10. Correlation (left) and ratio of standard deviations (right) of the modelled and observed time series of total seasonal pollen amounts from 2005 to 2011. Only stations with at least 5 years of observations are plotted.

Good model results in Central Europe confirm that the dense EAN network in the western ragweed colony was sufficient for accurate source calibration. This, however, is not unequivocal for the case of the eastern colony, where just a few sites were available with limited temporal coverage. The data were still sufficient to highlight this region as the most contaminated area and the largest ragweed pollen source in Europe. However, the details of the plant spread there were not fully understood.

5.4. Trends and intra-seasonal variability

The current model version considers the total seasonal emission (Fig. 2, left) as constant across years. This is the limitation of the calibration procedure based on total seasonal counts averaged over 7 years: it registers only the long-term signal in the emission accuracy. As a result, the model somewhat underestimates the dynamic range of the total seasonal values (Fig. 10, right; example time series for Hungary in Fig. 11). Improvements could be obtained by calibrating on annual basis, but for a forecasting model such parameterization is not possible (the total seasonal count is obviously not available until the season is over).

Computing the total emitted pollen amounts as a function of local meteorology (temperature, solar radiation, soil moisture, etc. during the growth period) could improve the model's ability to capture the year-to-year variability in pollen loads in the main source regions, which is currently under-predicted. For instance, the 2007 low total pollen count in Hungary (Fig. 11) can be related to an anomalously dry summer.

More generally, one can consider separately the invasion- and climate-related trends in total counts and the variability of the plant productivity due to specific features of that season. Such an analysis, however, has to be made with care; as seen from Fig. 11, a substantial part of the apparent trend in Hungary during the years under consideration was reproduced by SILAM even with a constant emission map. This is not surprising since the 7-year period is quite short and thus all apparent trends cannot be considered reliable. They might be caused by differences in precipitation, wind speed, mixing conditions, etc. during the flowering season. These factors are all included in the dispersion model. High correlations of the observed and modelled 7-year time series of total seasonal counts in Hungary (Fig. 10, left panel) show that in that region the year-to-year variability of pollen concentration is largely explained by these meteorological factors. The lower correlations in other regions (Ukraine, Milan and Lyon areas) indicate that the variability in those regions is rather the result of processes not currently covered by the model. For example, practically unpredictable but potentially strong regional impacts could be caused by eradication efforts and changes in agricultural practices.

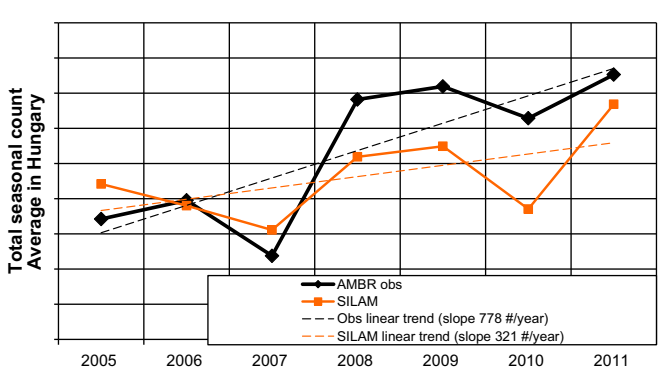

Fig. 11. Total seasonal pollen count, average over Hungarian stations [pollen day m^{-3}].

5.5. Model sustainability in the future climate

In the future, major changes can be expected in the distribution of ragweed habitat (Bullock et al., 2012; Cunze et al., 2013) due to changes in climate and land use (Rounsevell et al., 2006). The model developed here, when coupled with an external ecological model of ragweed spread, is capable of simulating the ragweed invasion and impacts in a changing climate. This is beyond the scope of the current paper, but will be an important area of future research for planning public health responses to ragweed's ongoing invasion.

Regarding the ragweed source term and SILAM itself, the most-important flowering parameters are related to day length, which is not affected by climate change. In the short term, the phenological model has proven to be not very sensitive to the temperature-related parameters. However, in Ziska et al. (2011), the lengthening of the ragweed pollen season has been connected with the warming trends and delayed frosts in autumn. If applied to climatically relevant timescales, SILAM is expected to reproduce such effects in northern areas, where the end of the flowering season is controlled by daily mean temperatures and frost.

The changes in climate are expected to be relevant for the seasonal pollen amount, which in SILAM is taken into account through the climate suitability index predicted by the external ecological model.

Finally, the transport modules are tested over the whole globe and shown to be robust to a wide range of atmospheric conditions (Sofiev et al., 2011).

6. Conclusions

An operational forecast model has been developed for the emission and atmospheric transport of ragweed pollen in Europe. The

model incorporates the main processes that influence ragweed pollen concentration in the atmosphere: phenological development of the plant, pollen release from the inflorescences, its transport by wind, mixing by turbulence, deposition via sedimentation and scavenging by precipitation.

The model has been compared with European aerobiological observations of *Ambrosia* pollen and was shown to reproduce the main features of the season in Europe, capturing both the spatial and temporal patterns in pollen air concentrations. For instance, the hit rate exceeded 0.8 in the main source regions for the exceedances of allergy-relevant concentration thresholds (5 and 20 pollen per m^3). The false alarm ratio stayed below 10%.

The application of the new model has produced the first European-scale simulation of ragweed pollen concentrations. The model outlined the areas of significant probability of exceedances of allergy-relevant thresholds. This showed that the strong south–north gradient of ragweed presence and prevailing west-to-east transport direction, together with natural barriers for pollen dispersion, such as mountains, reduced ragweed pollen levels in northern and western-most parts of Europe. However, the mechanistic modelling also highlighted the important role of long-range atmospheric transport in forming the high-concentration patterns. Due to long-range transport episodes of high concentrations can be recorded virtually anywhere in Europe, summing up to several days of harmful pollen levels per year even in regions remote from the heavily invaded areas. As such, our modelling illustrates the potential for a relatively localized invasive species to produce impacts on human health at a continental scale.

Acknowledgments

The study was funded by the European Commission under ENV.B2/ETU/2010/0037 “Assessing and controlling the spread and the effects of common ragweed in Europe”. Ragweed pollen information was kindly provided by the European Aeroallergen Network EAN (https://ean.polleninfo.eu/Ean; http://www.polleninfo.org). Support of FP7 projects HIALINE, MACC, and PASODOBLE is highly appreciated.

References

Bartková-Scevková, J., 2003. The influence of temperature, relative humidity and rainfall on the occurrence of pollen allergens (*Betula*, Poaceae, *Ambrosia artemisiifolia*) in the atmosphere of Bratislava (Slovakia). Int. J. Biometeorol. 48, 1–5.

Baskin, J.M., Baskin, C.C., 1980. Ecophysiology of secondary dormancy in seeds of *Ambrosia artemisiifolia*. Ecology 61, 475–480.

Basky, Z., Magyar, D., 2008. Impact of indigenous aphids on development of the invasive common ragweed (*Ambrosia artemisiifolia* L.) in Hungary. J. Pest Sci. 82, 19–25.

Bassett, I., Crompton, C., 1975. The biology of Canadian weeds: 11. *Ambrosia artemisiifolia* L. and *A. psilostachya* DC. Can. J. Plant Sci. 55, 463–476.

Belmonte, J., Vendrell, M., Roure, J.M., Vidal, J., Botey, J., Cadahia, A., 2000. Levels of *Ambrosia* pollen in the atmospheric spectra of Catalan aerobiological stations. Aerobiologia 16, 93–99.

Bullock, J.M., Chapman, D., Schafer, S., Roy, D., Girardello, M., Haynes, T., Beal, S., Wheeler, B., Dickie, I., Phang, Z., Tinch, R., Čivić, K., Delbaere, B., Jones-Walters, L., Hilbert, A., Schrauwen, A., Prank, M., Sofiev, M., Niemelä, S., Räisänen, P., Lees, B., Skinner, M., Finch, S., Brough, C., 2012. Assessing and controlling the spread and the effects of common ragweed in Europe. Final Report to the European Commission, DG Environment. NERC Centre for Ecology and Hydrology, https://circabc.europa.eu/sd/d/d1ad57e8-327c-4fdd-b908-dadd5b859eff/Final_Final_Report.pdf

Burbach, G.J., Heinzerling, L.M., Röhnelt, C., Bergmann, K.-C., Behrendt, H., Zuberbier, T., 2009. Ragweed sensitization in Europe – GA2LEN study suggests increasing prevalence. Allergy 64, 664–665.

Buters, J.T.M., Thibaudon, M., Smith, M., Kennedy, R., Rantio-Lehtimäki, A., Albertini, R., Reese, G., Weber, B., Galan, C., Brandao, R., Antunes, C.M., Jäger, S., Berger, U., Celenk, S., Grewling, Ł., Jackowiak, B., Sauliene, I., Weichenmeier, I., Pusch, G., Sarioglu, H., Ueffing, M., Behrendt, H., Prank, M., Sofiev, M., Cecchi, L., 2012. Release of Bet v 1 from birch pollen from 5 European countries. Results from the HIALINE study. Atmos. Environ. 55, 496–505.

Chauvel, B., Dessaint, F., Cardinal-Legrand, C., Bretagnolle, F., 2006. The historical spread of *Ambrosia artemisiifolia* L. in France from herbarium records. J. Biogeogr. 33, 665–673.

Chen, H., Chen, L., Albright, T.P., 2007. Predicting the potential distribution of invasive exotic species using GIS and information-theoretic approaches: a case of ragweed (*Ambrosia artemisiifolia* L.) distribution in China. Chin. Sci. Bull. 52, 1223–1230.

Cunze, S., Leiblein, M.C., Tackenberg, O., 2013. Range expansion of *Ambrosia artemisiifolia* in Europe is promoted by climate change. ISRN Ecol. 2013, 1–9.

D'Amato, G., Cecchi, L., Bonini, S., Nunes, C., Annesi-Maesano, I., Behrendt, H., Liccardi, G., Popov, T., Van Cauwenberge, P., 2007. Allergenic pollen and pollen allergy in Europe. Allergy 62, 976–990.

Dahl, Å., Strandhede, S.-O., Wihl, J.-A., 2000. Ragweed – an allergy risk in Sweden? Aerobiologia 15, 293–297.

Dechamp, C., Meon, H., 2009. *Ambrosia artemisiifolia* L. an invasive weed in metropolitain France: the geographical distribution before 2009. Ambrosie First Int. Ragweed Rev. 26, 110–120.

Dechamp, C., Meon, H., Reznik, S.Y., 2009. *Ambrosia artemisiifolia* L. an invasive weed in Europe and adjacent countries: the geographical distribution (except France) before 2009. Ambrosie First Int. Ragweed Rev. 26, 24–46.

Deen, W., Hunt, L.A., Swanton, C.J., 1998. Photothermal time describes common ragweed (*Ambrosia artemisiifolia* L.) phenological development and growth. Weed Sci. 46, 561–568.

Deen, W., Swanton, C.J., Hunt, L.A., 2001. A mechanistic growth and development model of common ragweed. Weed Sci. 49, 723–731.

Efstathiou, C., Isukapalli, S., Georgopoulos, P., 2011. A mechanistic modeling system for estimating large-scale emissions and transport of pollen and co-allergens. Atmos. Environ. 45, 2260–2276.

Essl, F., Dullinger, S., Kleinbauer, I., 2009. Changes in the spatio-temporal patterns and habitat preferences of *Ambrosia artemisiifolia* during its invasion of Austria. Presila, 119–133.

Fernández-Llamazares, Á., Belmonte, J., Alarcón, M., López-Pacheco, M., 2012. *Ambrosia*L. in Catalonia (NE Spain): expansion and aerobiology of a new bioinvader. Aerobiologia 28, 435–451.

Fumanal, B., Chauvel, B., Bretagnolle, F., 2007. Estimation of pollen and seed production of common ragweed in France. Ann. Agric. Environ. Med. 14, 233–236.

Galan, C., Antunes, C., Brandao, R., Torres, C., Garcia-Mozo, H., Caeiro, E., Ferro, R., Prank, M., Sofiev, M., Albertini, R., Berger, U., Cecchi, L., Celenk, S., Grewling, L., Jackowiak, B., Jäger, S., Kennedy, R., Rantio-Lehtimäki, A., Reese, G., Sauliene, I., Smith, M., Thibaudon, M., Weber, B., Weichenmeier, I., Pusch, G., Buters, J.T.M., Group, T.H., working, 2013. Airborne olive pollen counts are not representative of exposure to the major olive allergen Ole e 1. Allergy.

GISD, 2013. Global Invasive Species Database [WWW Document]. *Ambrosia* artemisiifolia., URL http://www.issg.org/database/species/ecology.asp?si=1125&fr=1&sts=sss&lang=EN (accessed 05.20.13).

Helbig, N., Vogel, B., Vogel, H., Fiedler, F., 2004. Numerical modelling of pollen dispersion on the regional scale. Aerobiologia 20, 3–19.

Hodisan, N., Morar, G., 2008. The spread of the invasive species *Ambrosia artemisiifolia* L. in Romania, between 2005–2007. Bull. Univ. Agric. Sci. Vet. Med. Cluj-Napoca Agric. 65, 129–134.

Huijnen, V., Eskes, H.J., Poupkou, A., Elbern, H., Boersma, K.F., Foret, G., Sofiev, M., Valdebenito, A., Flemming, J., Stein, O., Gross, A., Robertson, L., D'Isidoro, M., Kioutsioukis, I., Friese, E., Amstrup, B., Bergstrom, R., Strunk, A., Vira, J., Zyryanov, D., Maurizi, A., Melas, D., Peuch, V.-H., Zerefos, C., 2010. Comparison of OMI NO2 tropospheric columns with an ensemble of global and European regional air quality models. Atmos. Chem. Phys. 10, 3273–3296.

Jäger, S., 2000. Ragweed (*Ambrosia*) sensitisation rates correlate with the amount of inhaled airborne pollen. A 14-year study in Vienna, Austria. Aerobiologia 16, 149–153.

Jato, V., Rodríguez-Rajo, F.J., Alcázar, P., De Nuntiis, P., Galán, C., Mandrioli, P., 2006. May the definition of pollen season influence aerobiological results? Aerobiologia 22, 13–25.

Laaidi, M., Laaidi, K., Besancenot, J.P., M T., 2003a. Ragweed in France: an invasive plant and its allergenic pollen. Ann. Allergy Asthma Immunol. 91, 195–201.

Laaidi, M., Thibaudon, M., Besancenot, J.-P., 2003b. Two statistical approaches to forecasting the start and duration of the pollen season of *Ambrosia*in the area of Lyon (France). Int. J. Biometeorol. 48, 65–73.

Makra, L., Juhász, M., Béczi, R., Borsos, E., 2005. The history and impacts of airborne *Ambrosia*(Asteraceae) pollen in Hungary. Grana 44, 57–64.

Makra, L., Matyasovszky, I., Paldy, A., Deak, A.J., 2012. The influence of extreme high and low temperatures and precipitation totals on pollen seasons of *Ambrosia*, Poaceae and *Populus* in Szeged, southern Hungary. Grana 51, 215–227.

Makra, L., Matyasovszky, I., Thibaudon, M., Bonini, M., 2011. Forecasting ragweed pollen characteristics with nonparametric regression methods over the most polluted areas in Europe. Int. J. Biometeorol. 55, 361–371.

Mandrioli, P., Caneva, G., Sabbioni, C., 2003. Cultural Heritage and Aerobiology: Methods and Measurement Techniques for Biodeterioration Monitoring. Kluwer, Dordrecht.

Martin, M.D., Chamecki, M., Brush, G.S., 2010. Anthesis synchronization and floral morphology determine diurnal patterns of ragweed pollen dispersal. Agric. Forest Meteorol. 150, 1307–1317.

Mátyás, K.K., Vignesh, M.J.T., 2012. Population genetic analysis of common ragweed (*Ambrosia artemisiifolia* L.) in the Carpathian-basin [in Hungarian]. Magyar Gyomkutatás és Technológia. Hung. Weedresearch Technol. 13, 21–36.

Oswalt, M.L., Marshall, G.D., 2008. Ragweed as an example of worldwide allergen expansion. Allergy Asthma Clin. Immunol. 4, 130–135.

Pauling, A., Rotach, M.W., Gehrig, R., Clot, B., 2012. A method to derive vegetation distribution maps for pollen dispersion models using birch as an example. Int. J. Biometeorol. 56, 949–958.
Peternel, R., Čulig, J., Hrga, I., Hercog, P., 2006. Airborne ragweed (*Ambrosia artemisiifolia* L.) pollen concentrations in Croatia, 2002–2004. Aerobiologia 22, 161–168.
Pinke, G., Karacsony, P., Czucz, B., Botta-Dukat, Z., 2011. Environmental and land-use variables determining the abundance of *Ambrosia artemisiifolia* in arable fields in Hungary. Preslia 83, 219–235.
Piotrowska, K., Weryszko-Chmielewska, E., 2006. *Ambrosia* pollen in the air of Lublin, Poland. Aerobiologia 22, 149–156.
Ranta, H., Siljamo, P., Oksanen, A., Sofiev, M., Linkosalo, T., Bergmann, K.-C., Bucher, E., Ekebom, A., Emberlin, J., Gehrig, R., Hallsdottir, M., Jato, V., Jäger, S., Myszkowska, D., Paldy, A., Ramfjord, H., Severova, E., Thibaudon, M., 2011. Aerial and annual variation of birch pollen loads and a modelling system for simulating and forecasting pollen emissions and transport at an European scale. Aerobiol. Monogr. 1, 115–131.
Raynor, G.S., Ogden, E.C., Hayes, J.V., 1970. Dispersion and deposition of ragweed pollen from experimental sources. J. Clim. Appl. Meteorol. 9, 885–895.
Reznik, S.Y., 2009. Common ragweed (*Ambrosia artemisiifolia* L.) in Russia: spread, distribution, abundance, harmfulness and control measures. Ambroisie First Int. Ragweed Rev., 26.
Ridolo, E., Albertini, A., Giordano, D., Soliani, L., Usberti, I., Dall'Aglio, P.P., 2006. Airborne Pollen Concentrations and the Incidence of Allergic Asthma and Rhinoconjunctivitis in Northern Italy from 1992 to 2003. Int. Arch. Allergy Immunol. 20, 142.
Rodinkova, V., Palamarchuk, O., DuBuske, L.M., 2012. The most abundant Ambrosia pollen count is associated with the southern, eastern and the northern-eastern Ukraine. Alergol. Immunol. 9, 156.
Rouïl, L., Beekman, M., Foret, G., Sofiev, M., Vira, J., 2008. Assessment Report: Air quality in Europe in 2008. Reading, MACC: Monitoring Atmospheric Composition & Climate.
Rouïl, L., Beekman, M., Foret, G., Sofiev, M., Vira, J., 2009. Assessment Report: Air quality in Europe in 2009. Reading, MACC: Monitoring Atmospheric Composition & Climate.
Rounsevell, M.D.a., Reginster, I., Araújo, M.B., Carter, T.R., Dendoncker, N., Ewert, F., House, J.I., Kankaanpää, S., Leemans, R., Metzger, M.J., Schmit, C., Smith, P., Tuck, G., 2006. A coherent set of future land use change scenarios for Europe. Agric. Ecosyst. Environ. 114, 57–68.
Rybncek, O., Jäger, S., 2001. *Ambrosia* (ragweed) in Europe. Allergy Clin. Immunol. Int. 13, 60–66.
Saar, M., Gudžinskas, Z., Plompuu, T., Linno, E., 2000. Ragweed plants and airborne pollen in the Baltic states. Aerobiologia 16, 101–106.
Šaulienė, I., Gudžinskas, Z., Veriankaitė, L., Malciūtė, A., Leščiauskienė, V., 2011. Distribution of *Ambrosia* plants and airborne pollen in Lithuania. Food Agric. Environ. 9, 547–550.
Šaulienė, I., Veriankaitė, L., Šaulys, A., 2012. Biometrical assessment of ragweed (*Ambrosia artemisiifolia* L.). Zemdirbystė 99, 319–326.
Severova, E., Volkova, O., 2012. Southern Russia as a source of *Ambrosia* pollen. In: Proc. of Firth European Symposium on Aerobiology.
Šikoparija, B., Skjøth, C.a.A., Kübler, K.A., Dahl a. Sommer, J., Grewling, Ł., Radišić, P., Smith, M., Alm Kübler, K., Dahl a. Sommer, J., Grewling, Ł., Radišić, P., Smith, M., 2013. A mechanism for long distance transport of *Ambrosia*pollen from the Pannonian Plain. Agric. Forest Meteorol. 180, 112–117.
Šikoparija, B., Smith, M., Skjøth, C.A., Radišić, P., 2009. The Pannonian plain as a source of *Ambrosia* pollen in the Balkans. Int. J. Biometeorol., 263–272.
Siljamo, P., Sofiev, M., Filatova, E., Grewling, L., Jäger, S., Khoreva, E., Linkosalo, T., Ortega Jimenez, S., Ranta, H., Rantio-Lehtimäki, A., Svetlov, A., Veriankaite, L., Yakovleva, E., Kukkonen, J., 2013. A numerical model of birch pollen emission and dispersion in the atmosphere. Model evaluation and sensitivity analysis. Int. J. Biometeorol. 57, 125–136.
Siljamo, P., Sofiev, M., Severova, E., Ranta, H., Kukkonen, J., Polevova, S., Kubin, E., Minin, A., 2008. Sources, impact and exchange of early-spring birch pollen in the Moscow region and Finland. Aerobiologia 24, 211–230.
Simpson, M., 2011. Determining the potential distribution of highly invasive plants in the Carpathian Mountains of Ukraine: a species distribution modeling approach under different climate-land-use scenarios and possible implications for natural-resource management.
Skjøth, C.A., Smith, M., Šikoparija, B., Stach, A., Myszkowska, D., Kasprzyk, I., Radišić, P., Stjepanović, B., Hrga, I., Apatini, D., 2010. A method for producing airborne pollen source inventories: an example of *Ambrosia*(ragweed) on the Pannonian Plain. Agric. Forest Meteorol. 150, 1203–1210.
Smith, M., Skjøth, C.A., Myszkowska, D., Uruska, A., Puc, M., Stach, A., Balwierz, Z., Chlopek, K., Piotrowska, K., Kasprzyk, I., Brandt, J., 2008. Long-range transport of *Ambrosia* pollen to Poland. Environ. Res. 148, 1402–1411.
Smolik, M.G., Dullinger, S., Essl, F., Kleinbauer, I., Leitner, M., Peterseil, J., Stadler, L.-M., Vogl, G., 2010. Integrating species distribution models and interacting particle systems to predict the spread of an invasive alien plant. J. Biogeogr. 37, 411–422.
Sofiev, M., Bergmann, K.-C. (Eds.), 2013. Allergenic Pollen. Springer.
Sofiev, M., Galperin, M., Genikhovich, E., 2008. A Construction and evaluation of eulerian dynamic core for the air quality and emergency modelling system SILAM. In: Borrego, C., Miranda, A.I. (Eds.), Air Pollution Modeling and Its Application XIX. Springer, Netherlands, pp. 699–701.
Sofiev, M., Siljamo, P., Ranta, H., Linkosalo, T., Jaeger, S., Rasmussen, A., Rantio-Lehtimaki, A., Severova, E., Kukkonen, J., 2013. A numerical model of birch pollen emission and dispersion in the atmosphere. Description of the emission module. Int. J. Biometeorol. 57, 45–48.
Sofiev, M., Siljamo, P., Ranta, H., Rantio-Lehtimäki, A., 2006. Towards numerical forecasting of long-range air transport of birch pollen: theoretical considerations and a feasibility study. Int. J. Biometeorol. 50, 392–402.
Sofiev, M., Soares, J., Prank, M., De Leeuw, G., Kukkonen, J., 2011. A regional-to-global model of emission and transport of sea salt particles in the atmosphere. J. Geophys. Res. 116, 25.
Solazzo, E., Bianconi, R., Pirovano, G., Matthias, V., Vautard, R., Moran, M.D., Wyat Appel, K., Bessagnet, B., Brandt, J., Christensen, J.H., Chemel, C., Coll, I., Ferreira, J., Forkel, R., Francis, X.V., Grell, G., Grossi, P., Hansen, A.B., Miranda, A.I., Nopmongcol, U., Prank, M., Sartelet, K.N., Schaap, M., Silver, J.D., Sokhi, R.S., Vira, J., Werhahn, J., Wolke, R., Yarwood, G., Zhang, J., Rao, S.T., Galmarini, S., 2012a. Operational model evaluation for particulate matter in Europe and North America in the context of AQMEII. Atmos. Environ. 53, 75–92.
Solazzo, E., Bianconi, R., Vautard, R., Appel, K.W., Moran, M.D., Hogrefe, C., Bessagnet, B., Brandt, J., Christensen, J.H., Chemel, C., Coll, I., Denier van der Gon, H., Ferreira, J., Forkel, R., Francis, X.V., Grell, G., Grossi, P., Hansen, A.B., Jeričević, A., Kraljević, L., Miranda, A.I., Nopmongcol, U., Pirovano, G., Prank, M., Riccio, A., Sartelet, K.N., Schaap, M., Silver, J.D., Sokhi, R.S., Vira, J., Werhahn, J., Wolke, R., Yarwood, G., Zhang, J., Rao, S.T., Galmarini, S., 2012b. Model evaluation and ensemble modelling of surface-level ozone in Europe and North America in the context of AQMEII. Atmos. Environ. 53, 60–74.
Stach, A., Smith, M., Skjøth, C.A., Brandt, J., 2007. Examining *Ambrosia* pollen episodes at Poznań (Poland) using back-trajectory analysis. Int. J. Biometeorol., 275–286.
Stark, P.C., Ryan, L.M., McDonald, J.L., Burge, H.A., 1997. Using meteorologic data to predict daily ragweed pollen levels. Aerobiologia 13, 177–184.
Taramarcaz, P., Lambelet, B., Clot, B., Keimer, C., Hauser, C., 2005. Ragweed (*Ambrosia*) progression and its health risks: will Switzerland resist this invasion? Swiss Med. Wkly. 135, 538–548.
Turos, O.I., Kovtunenko, I.N., Markevych, Y.P., Drannik, G.N., DuBuske, L.M., Marzeyev, O., 2009. Aeroallergen monitoring in Ukraine reveals the presence of a significant ragweed pollen season. J. Allergy Clin. Immunol. 123, 358.
Veriankaitė, L., Siljamo, P., Sofiev, M., Šaulienė, I., Kukkonen, J., 2009. Modelling analysis of source regions of long-range transported birch pollen that influences allergenic seasons in Lithuania. Aerobiologia 26, 47–62.
Vinogradova, Y.R., Majorov, S.R., Khorun, L.V., 2010. Black Book of Central Russia: Alien Species of flora of Central Russia (in Russian). GEOS, Moscow.
Yankova, R., Zlatev, V., Baltadjieva, D., 2000. Quantitative dynamics of *Ambrosia* pollen grains in Bulgaria. Aerobiologia 16, 299–301.
Zink, K., Vogel, H., Vogel, B., Magyar, D., Kottmeier, C., 2012. Modeling the dispersion of *Ambrosia artemisiifolia* L. pollen with the model system COSMO-ART. Int. J. Biometeorol. 56, 669–680.
Ziska, L., Knowlton, K., Rogers, C., Dalan, D., Tierney, N., Elder, M.A., Filley, W., Shropshire, J., Ford, L.B., Hedberg, C., Fleetwood, P., Hovanky, K.T., Kavanaugh, T., Fulford, G., Vrtis, R.F., Patz, J., a Portnoy, J., Coates, F., Bielory, L., Frenz, D., 2011. Recent warming by latitude associated with increased length of ragweed pollen season in central North America. Proc. Natl. Acad. Sci. U.S.A. 108, 4248–4251.